Award Number DE-EE0005274 Final Report
Performing Organization University of Rochester
PI Lewis Rothberg (Phone 585-273-4725, FAX 585-276-0205)
Title Efficient Light Extraction from Organic Light-Emitting Diodes Using Plasmonic Scattering Layers
Reporting Period – October 1, 2011 – November, 30, 2012

I. Context

Our project addressed the DOE MYPP 2020 goal to improve light extraction from organic light-emitting diodes (OLEDs) to 75% (Core task 6.3). As noted in the 2010 MYPP, "the greatest opportunity for improvement is in the extraction of light from [OLED] panels". There are many approaches to avoiding waveguiding limitations intrinsic to the planar OLED structure including use of textured substrates, microcavity designs and incorporating scattering layers into the device structure. We have chosen to pursue scattering layers since it addresses the largest source of loss which is waveguiding in the OLED itself. Scattering layers also have the potential to be relatively robust to color, polarization and angular distributions. We note that this can be combined with textured or microlens decorated substrates to achieve additional enhancement.

II. Concept and technical approach

We have chosen to use silver nanoparticles as our scatterers for several reasons. They have the largest scattering per unit volume of any known material and are easily processed since their surfaces are straightforward to chemically functionalize. The main fundamental drawback of silver nanoparticles is that they can absorb as well as scatter light. An additional problem of a non-fundamental nature arises from the need to make planar OLED devices ~ 100nm thick compatible with nanotextured silver so that a suitable planarization step must be added to device fabrication.

The overall approach can be summarized by the diagram of Figure 1 where a plasmonic scattering layer containing silver particles is integrated with a standard state-of-the-art OLED. Our program therefore involves the following components: (1) Modeling of silver nanoparticle scattering layers, (2) Synthesis of silver nanoparticles, (3) Assembly of silver nanoparticle assemblies, (4) Planarization of the scattering layer and (5) Growth of OLEDs on the planarization layers.

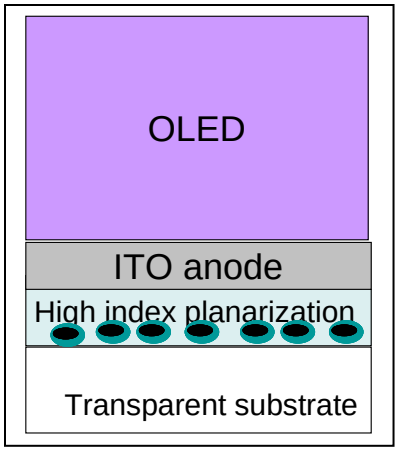

Figure 1. OLED with plasmonic scatterer extraction layer.

III. Program milestones and progress

Our original Table of milestones and success criteria from the original proposal is reproduced here for completeness.

Milestone	Month	Description of activities*	Success criteria
1	3	FDTD study of silver nanorods	Calculated scattering spectra and cross-sections with caps and encapsulation
2	4	Synthesis of silver nanorods	Library covering 450 – 700 nm
3	6	Capped silver nanorods	Library covering 450 – 700 nm
4	9	Assemblies of capped silver nanorods using electrostatics	2-D and 3-D structures with controllable OD 0.1 –0.5 flat across visible to +/- 0.1
5	12	FDTD study of capped nanorod assemblies	Predicted scattering behavior of assemblies as a function of loading and mixture
6	12	Planarization/encapsulation of capped nanorod assemblies	High index planarization suitable and growth of high conductivity ITO electrodes on top
7	15	Complete study of alternative silver deposition protocols and TiO_2 benchmark	Plasmonic layers to be evaluated in optical and device studies for comparison
8	18	Optical studies of total internal reflection suppression by nanorod assemblies	Conclusions about optimal scattering layers for device integration, 3.5X extraction enhancement over 450-700 nm with single layers
9	21	Bottom-emitting white OLEDs suitable for extraction studies	White OLEDs with > 1000 hour operational stability for scattering layer tests
10	21	Top-emitting white OLEDs suitable for extraction studies	White OLEDs with > 1000 hour operational stability for scattering layer tests
11	24	Integration of scattering layers with bottom-emitting devices	Reproducible fabrication process incorporating controls for evaluation of scattering enhancement, first results
12	24	Integration of scattering layers with top-emitting devices	Reproducible fabrication process incorporating controls for evaluation of scattering enhancement, first results
13	30	Evaluation of scattering layers in bottom- and top-emitting devices	Data for extraction efficiency, color balance, angular distribution
14	30	Demonstration of stable top- and bottom-emitting white OLEDs with plasmonic scattering layers	White OLEDs with > 5000 hour operational stability (LM50)
15	36	Optimization of color balance and fabrication process	State-of-the-art top and bottom-emitting white OLEDs with 70% extraction efficiency and good color balance
Notes:		* Many of the activities, including device fabrication, are ongoing. Milestone refers to first completion of task.	

However, the project management plan was substantially modified in January 2012 and again in May 2012 to reflect DOE feedback and technical learnings in the program. The DOE feedback was based upon the assertion that meeting our original milestones would not demonstrate project feasibility (i.e. improved extraction from OLEDs) by the end of year 1. It was therefore recommended to reconfigure the program to accelerate device studies that demonstrated the promise of the approach. Thus, efforts to make ellipsoidal silver nanoparticles (rods) with controllable plasmon resonance were postponed to year 2 while planarization and model structure and OLED fabrication were accelerated to year 1. It was felt quite sensibly that it would be better to demonstrate extraction enhancement first and to address spectral and angular balance later in the program. Our early modeling work also showed that spherical silver nanoparticles of large size (> 100 nm diameter) behave differently than smaller ones and exhibit very broad plasmon resonance nearly spanning the visible. Therefore, it would still be possible to demonstrate relatively broad spectral enhancement even without the originally proposed silver nanorod "library".

Our revised year 1 tasks and milestones correspond to working through the structure in Figure 1 and can be summarized as follows (with full detail and metrics in the most recent PMP):

1) Theoretical support for feasibility of 70% extraction
2) Synthesis of large spherical silver particles
3) Assembly of silver nanoparticles into layers with suitable optical density
4) Planarization of the silver nanoparticle layer with a flat, robust platform for OLED overgrowth
5) Growth of high quality ITO
6) Fabrication of optical structures and OLEDs that quantify extraction enhancement over controls

The remainder of the progress report below addresses our progress on these tasks individually after which we will discuss our plans for years 2 and 3 of the program.

A. Theoretical modeling and feasibility studies

Our original proposal contained a very simple model that could be used to estimate the potential extraction efficiency for light from OLEDs using scattering layers. The idea is that each scattering event leaves some probability of shifting the light into the fraction of solid angle in the escape cone which we assume to be $\eta = 1-(1-(n_{ext}/n_{int})^2)^{0.5}$. This takes on a value of 53% for escape from the emitter (n = 1.7) into the substrate (n = 1.5).

We can compute approximately the total fraction of light f escaping the device to be

$$f = \eta[1 + \Sigma ((1-\eta)^n R^n]$$

when we make the following assumptions:

1) Scattering by silver particles randomly redistributes the propagation direction of incident radiation.
2) A fraction of the light R is retained (i.e. not lost to absorption) at each scattering event.
3) Losses from reflection at the OLED cathode are negligible.
4) Light that is coupled into the substrate can be recovered with high efficiency using a brightness enhancement film or microlens treatment of the substrate.

If the fraction of light not absorbed upon scattering is R = 0.9, then f ~ 0.91 while even for modest R = 0.7, we can achieve f ~ 0.78.

Empirically, we believe that assumption #4 is sound. While we know that electrode loss (#3) is not negligible, best estimates place it at 3-8% and there are ways to modify the structure to reduce that number. The purpose of the theory is to test the first three assumptions, most particularly the first two.

We realized that we could calculate both the scattering fraction R and the angular distribution exactly using Mie theory if we confined our computations to spherical silver nanoparticles and the result is shown in Figure 2 which plots the absolute scattering cross-sections and the fraction of the extinction that is scattering which is called "Albedo" and is our theory parameter R for silver nanoparticles in air:

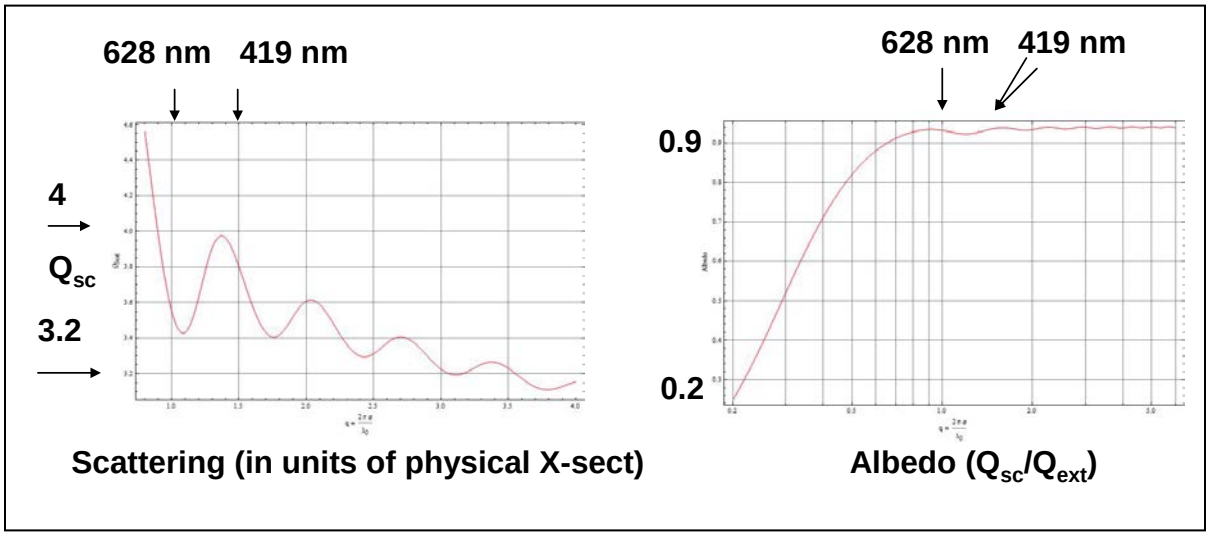

Figure 2: Absolute cross-section in units of physical cross-section $\pi d^2/4$ where d is the particle diameter (left). Fraction of light scattered relative to total extinction (right). The horizontal axis is in units of particle diameter relative to wavelength so that wavelength markers for d = 100 nm silver particles are labeled on the top axis for clarity.

The results of figure 2 prove that scattering cross-sections are very large and confirms that submonolayer coverages of silver nanoparticles will be adequate to form a strong scattering layer. The calculations also show that the fraction of light scattered R is well over 90% throughout the visible spectrum, validating assumption #2 of the model. Figure 3

complements these calculations with an assessment of angular distribution showing that it is very broad and validation assumption #1 of the model.

We have repeated these calculations using the more rigorous FDTD approach, showing that the Lumerical results closely match literature data for gold scattering in our annual report. We experimented with various literature dielectric functions for Ag and found the most reliable to be the data of Palik from Material Explorer on our Lumerical FDTD software. Using these data, we calculated scattering efficiency (i.e. how large the scattering cross-section is relative to physical size of the particles) and albedo, obtaining results similar those above obtained using Mie Theory. Sample results for a 200 nm diameter silver particle embedded in refractive index 1.8 material are shown in Figure 3:

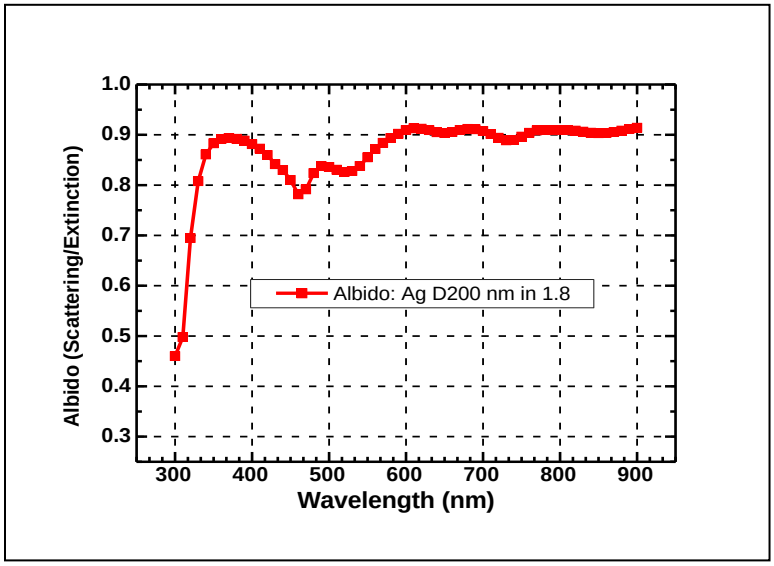

Figure 3a. Ratio of scattering to total extinction for 200 nm diameter silver spheres in a host medium with refractive index 1.8.

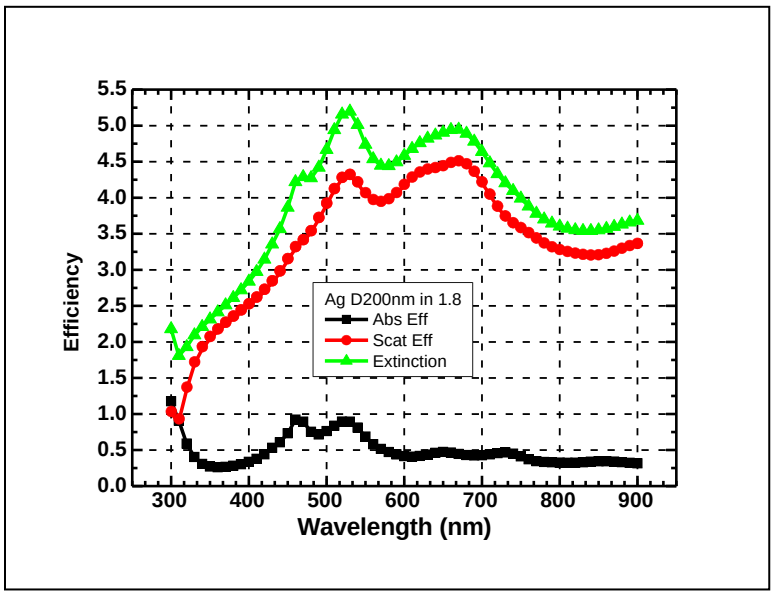

Figure 3b. Scattering cross-section of 200 nm diameter silver spheres in host medium of refractive index 1.8.

These data strongly support our second assumption, namely that large silver particles scatter with relatively low losses. Albedos of 90% would support 5 or 6 scattering events to try to funnel light into the escape cone.

We will show below that theory predicts moderate enhancements can be obtained with plasmonic scattering structures like those in Figure 1 but not nearly as high as predicted by our analytical theory above. It is our belief that the difference is traceable to a failure of the first assumption of the model, that of strong scattering which isotropically redistributes the scattered light.

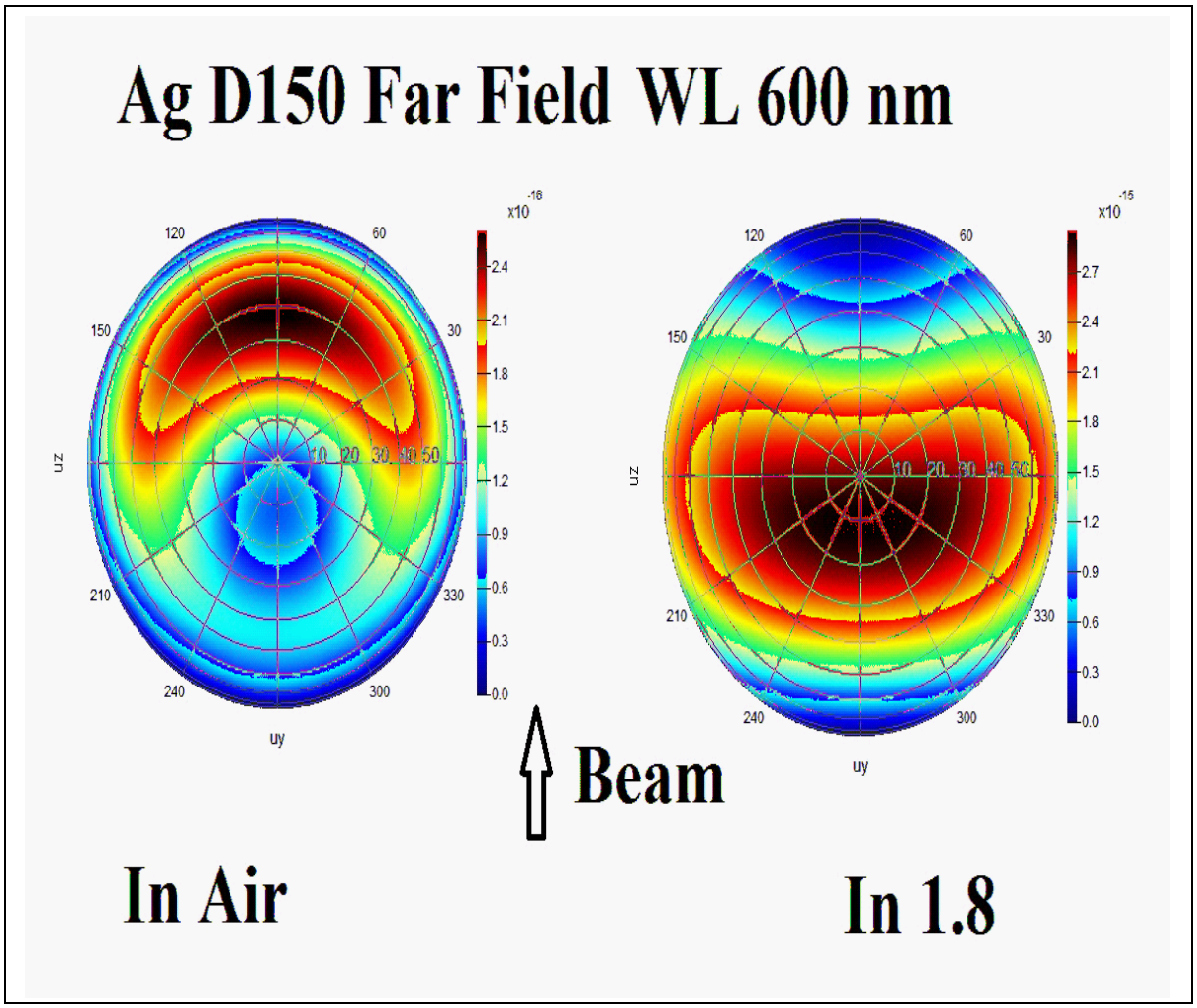

Figure 4. Angular distribution of scattering of 600 nm light using FDTD for large silver particles in air or embedded in material of refractive index 1.8.

As seen in Figure 4, the particles do cause strong redistribution of scattering angle. However, the particles in high refractive index preferentially back scatter which is not ideal since this tends to reduce the extraction efficiency of light within the escape cone. The width of the average angular deviation is around ±40 degrees which one might think enables efficient exchange of light between the angles where it is waveguided in the device and the escape cone. It is important to remember, however, that the scattering is a three dimensional problem and that the deviation angles are not necessarily in plane of incidence of the light at the escape interface. Thus, the ±40 degrees tends to overestimate the actual effectiveness of the scattering.

Having developed considerable confidence in the theory, we have applied it to full OLED device structures extensively to quantify enhancement. Several typical results are illustrated below. The general structure used to simulate the OLED is much like that of Figure 1 and is shown below. The calculation assumes periodic boundary conditions to make it tractable.

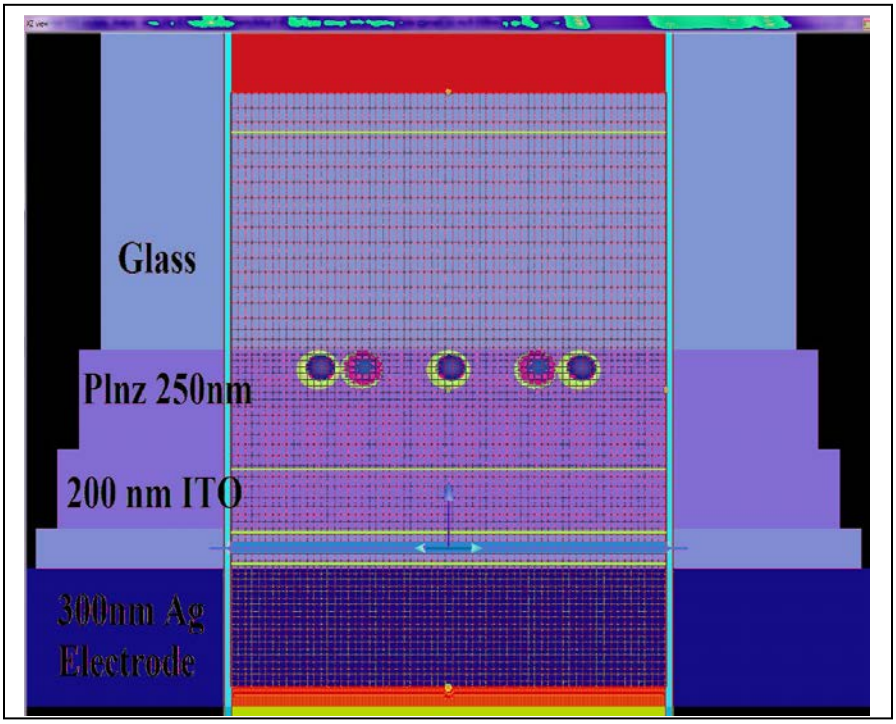

Figure 5: Two-dimensional view of our 3-D sample computational structure used to model light extraction from OLEDs using plasmonic (spherical Ag) scatterers. The particles are embedded in material of refractive index 2.1 that is closely matched to the ITO and planarized. The arrows indicate the location of the source in the emissive layer of the OLED (refractive index 1.7). An intensity monitor is placed in the glass substrate to measure the light extracted into the substrate from the device structure.

We use simulation regions of 1 μm x 1 μm x 1.5 μm. The source can be s or p-polarized and we will specify in our computations below. For technical reasons, the Lumerical software cannot create a correctly balanced three dimensional isotropic source so what we have done is to use plane wave sources at a large number of angles θ with respect to the surface normal and weighted their intensity by the $\sin^2\theta$ to quantify overall extraction efficiency. The mesh size has been reduced to be small enough so that the results are unaffected by mesh size. In the regions with the nanoparticles, this is ~ 1 nm so that the process is computationally intensive but easily accomplished on our supercomputer.

A few points about the structure are in order. First, we have used both “ideal”, silver and aluminum (i.e. LiF:Al) cathodes to understand the effects of cathode absorption on the process. We found that silver is noticeably better than aluminum as expected due to its much lower absorption but the largest part of the loss is in the plasmonic particles in each of these cases and so we do not need to consider the electrode loss. There are a substantial number of

important variables in constructing the model geometry and it is not simple to fully investigate all of them. Most important is the size, shape, placement and overall density of the scatterers. We have done a considerable amount of variation of size and overall density but much work remains to be done in terms of possible improvements to shape and placement. The refractive index of the planarization layer is also important as is the color and polarization of the light. We have done our best to sample the geometries that we think are practical to engineer in real devices but it is likely that our configurations can be improved, perhaps considerably.

Our initial work with Lumerical FDTD simply reproduced extraction efficiencies for OLEDs of the geometry in Figure 5 without scatterers and we obtained 19.2% into air and 53% into the substrate with ideally reflecting cathodes and slightly less with real cathodes. These are in good agreement with estimates based on simple calculations of the fraction of solid angle in the escape cones for the refractive indeces used. A typical set of data with plasmonic scatterers is presented in Figures 6a and 6b and is explained below. We really do mean "typical" and have seen geometries with better and worse extraction efficiencies.

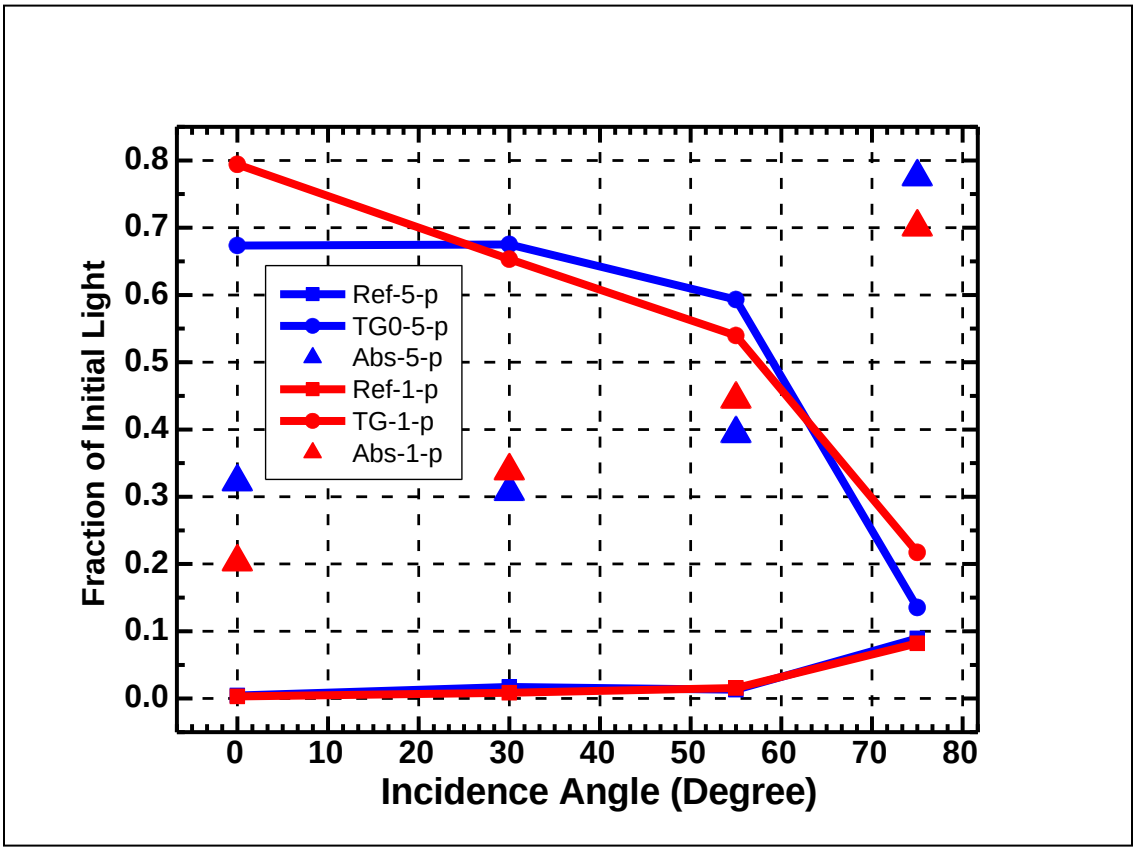

Figure 6a: Light extracted from an OLED device into glass like that of figure 5 as a function of angle. The scatterers are 200 nm spherical particles at around 15% coverage and the simulation uses p-polarized light. The angle for total internal reflection in the absence of the scatterers is ~ 62 degrees. The blue curves are for an irregular geometry and the red curves for a simple periodic geometry of scatterers at around the same coverage.

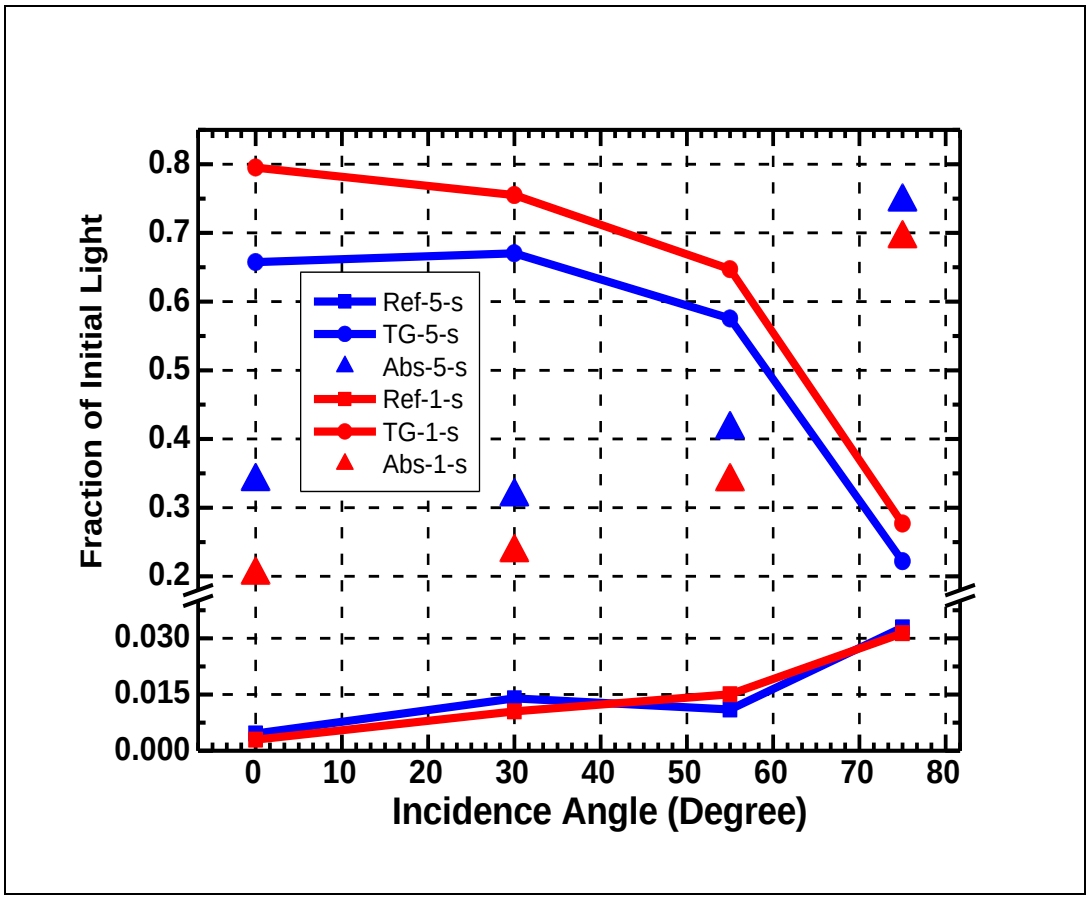

Figure 6b: Data analogous to those of Figure 6a but for s-polarized light.

The overall extraction efficiency is slightly improved relative to what is seen without plasmonic scatterers for s-polarized light and slightly worse for p-polarized light. The reason can be inferred from Figures 6a and 6b which is that ~ 20 to 30% of the 53% of the light in the cone that can escape into the substrate (initially < 62 degrees) is lost to absorption while ~25-35% of the 47% of the light that would have been waveguided (initially > 62 degrees) is extracted into the substrate. The reason that the s-polarized light is helped more by scattering is the absence of a Brewster angle in s-polarization. The Brewster angle means that p-polarized light is less impeded by internal reflections within the escape cone so that scattering to redistribute angles does not help as much.

So far our best theoretical result from the simulations is for 300nm diameter Ag spheres at ~ 14% coverage. We improve unpolarized light extraction into the substrate by around 7%. Ordinarily, we'd get around 95% into the 53% escape cone (0.504) and with the scatterers we can get ~ 75% of the 53% initially in the escape cone and 30% of the 47% out of the escape cone (0.538). It is important to note that this is at 600 nm but extraction slowly degrades towards the blue. It is surprising to us that such large particles appear to be optimal. We are optimistic that shapes of particles where the scattering is more preferentially forward and perhaps different particle distributions will show better results and we are working to identify

better geometries within the constraints of what we think we can produce synthetically. We are also modeling top emitting devices where the approach may work better if the engineering difficulties in making scatterers on top of the OLED can be managed. Our experimental efforts on extraction from fully operational OLEDs will be detailed in section F.

One final general theoretical result that we think is of interest is tracking the decay of the light field in the device with time (Figure 7). The field can decay due either to extraction or absorption but what these data tell us is whether the losses we have predicted are reasonable. As can be seen by a comparison of field retention at normal incidence and above the nominal critical angle, the field is rapidly extracted at normal incidence but has at least ~ 5 opportunities to be scattered into the escape cone. This is consistent with a loss per pass that accounts for silver scatterers with 90% albedo plus electrode loss. This is strong confirmation of our idea that we need better angular redistribution and more forward scattering in our scattering events so that we can extricate the light into the escape cone within ~ 5 passes.

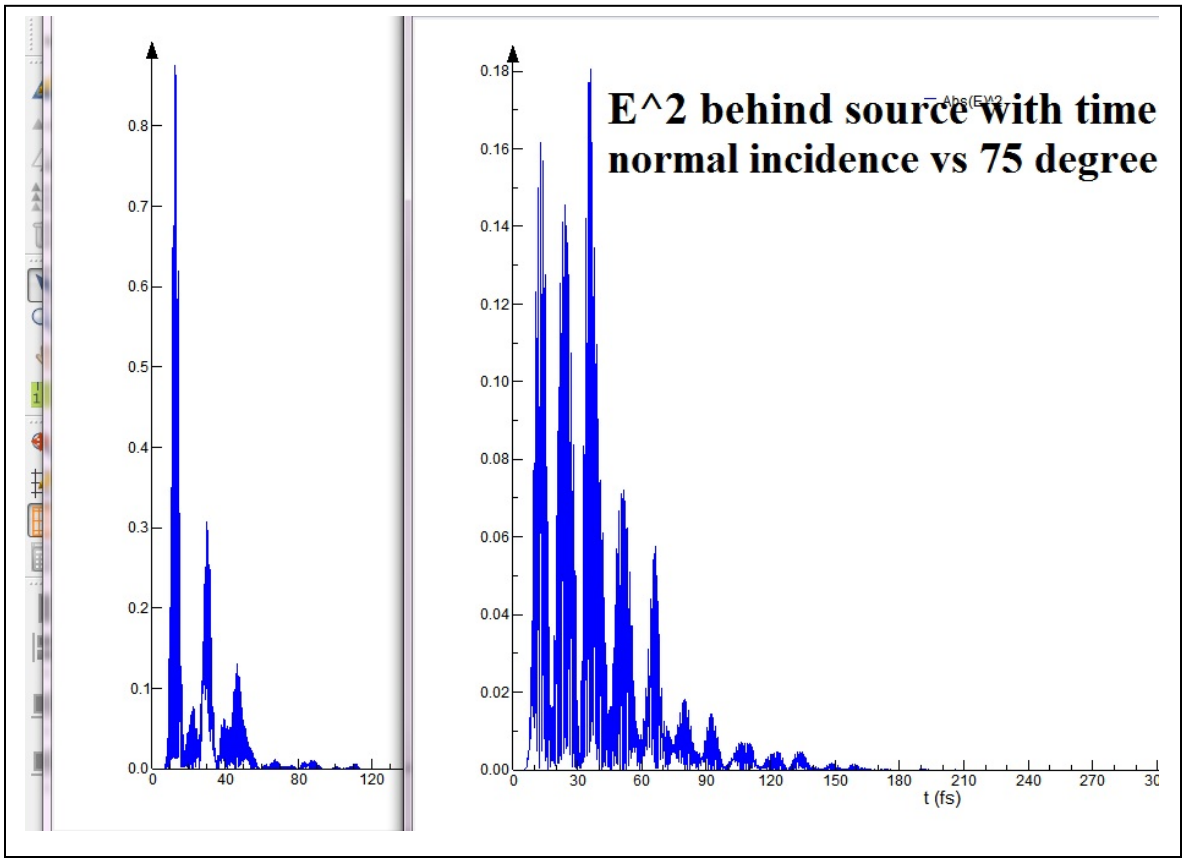

Figure 7. Field decay versus time for 600 nm emission in an OLED like that of Figure 1. At left is normal incidence where the field quickly escapes the OLED region and at right is above the critical angle where there are several bounces before the light is either absorbed (~70%) or scattered out (~30%) into the substrate.

B. Silver nanoparticle synthesis

As clear from the milestones Table, our original plan was to produce nanorod libraries. We were able to produce gold nanorods in high yield but our silver nanorod synthesis proved to be inefficient and did not produce uniform size and shape distributions. Even though we were able to produce silver with nice looking plasmon resonance (Figure 8), lack of control and reproducibility plagued us. For this reason, we contacted Vladimir Kitaev at the University of Waterloo who has published work where his group has succeeded in what we would like to do in January 2012. He kindly agreed to help us. However, as explained above, discussions with DOE convinced us to reprioritize the program so we postponed accepting Kitaev's offer until after our feasibility demonstration of extraction enhancement with silver spheres. The silver nanospheres of 100 nm diameter (corresponding to what the theory of Figure 2 suggests is an excellent choice) were easily synthesized by Chi-Sheng Chang in our group (Figure 9 left). These were made using standard reduction of Ag+ (from $AgNO_3$) by ascorbic acid using Gum Arabic as a surface stabilizer to suppress nanoparticle aggregation by imbuing the silver nanopheres with negative surface charge.

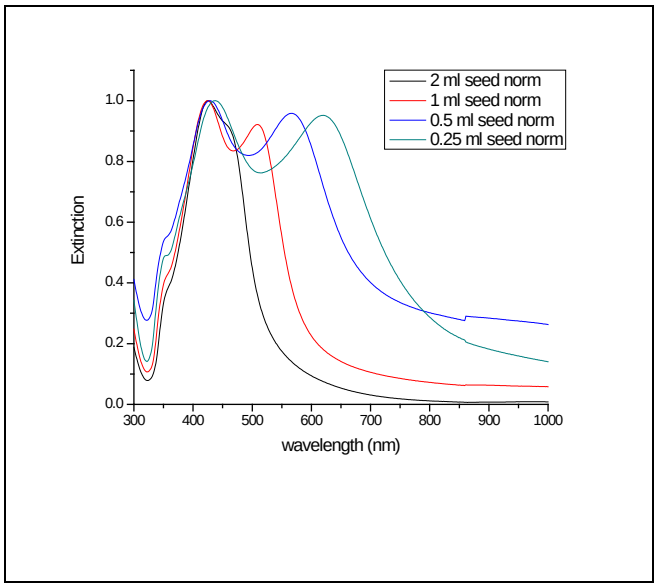

Figure 8. Extinction spectra for silver nanorod preparations of different aspect ratios.

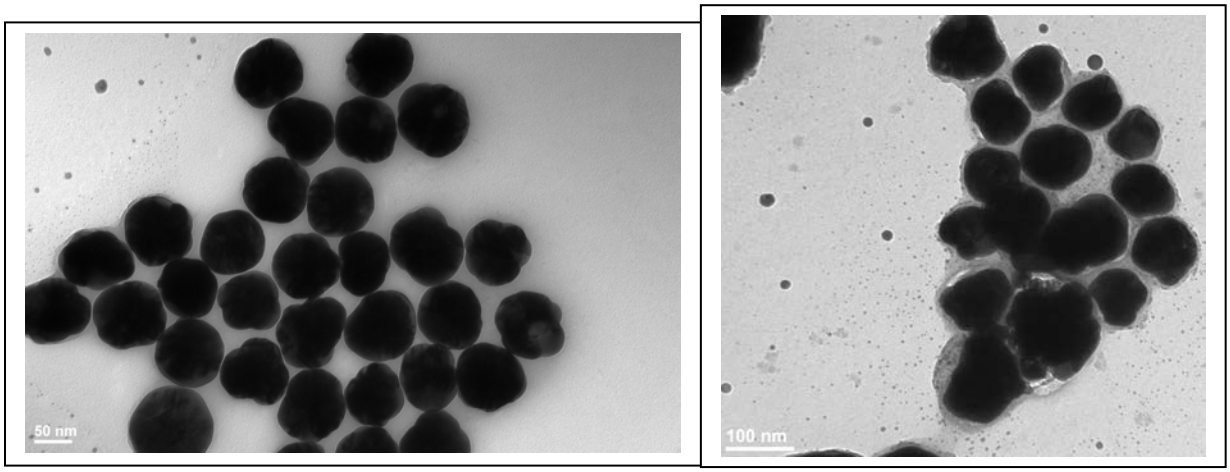

Figure 9. Scanning electron micrographs of silver nanospheres with ~100 nm diameter uncapped (left) and oxide capped (right)

Just as with gold nanorods, we were able to oxide cap the silver nanospheres since this may improve their processability (specifically ability to withstand heating when making ITO) and long term stability (Figure 9 right).

In summary, we have successfully synthesized and functionalized large (~100 nm diameter) silver nanospheres that can be assembled into plasmonic scattering layers (see section C below) adequate to meet our other milestones and to test the feasibility of efficient light extraction from OLEDs (see section F below). In consultation with DOE, we deferred our original goal to make "libraries" of silver nanorods with variable plasmon resonance since that addresses the second order issue of balancing extraction of various colors emitted from white OLEDs across the spectrum.

C. Self-assembly of large silver nanospheres

We have used a capping agent, Gum Arabic, to prevent aggregation of the nanoparticles. This has several purposes. First, the capping agent works by electrostatic repulsion (Gum Arabic carries a net negative charge) and the associated charge can be used to attract the nanoparticles to a substrate. Second, keeping the particles independent allows us to retain control over the plasmon resonance which changes substantially when particles pack densely and their charge densities interact.

We are able to make the surface charge of the substrate positive by functionalizing the glass with a monolayer of PVP (polyvinyl pyridine). Silver nanoparticles can be spontaneously deposited onto these subtrates in a controlled fashion to produce relatively uniform films with optical densities spanning the range set out in our metrics. A typical SEM is shown in Figure 10 (left) along with UV-visible extinction spectra (right) at several places on the (2"x 2") film to demonstrate macroscopic uniformity. It is gratifying that the coverage estimated from the SEM along with the theory (see section A, Figure 2) showing that 100 nm silver nanospheres scatter with ~ 4 times their physical cross-section lead to estimated optical densities consistent with the UV-visible measurement. Indeed, the extinction spectrum also

looks to be in good qualitative agreement with the spectral calculations (Figure 3) and has substantial scattering across the entire spectral region of interest to us for the light extraction application. The coverage illustrated on the SEM is also close to that in our modeling (Figures 6 and 7) and what we believe to be ideal although it is clear from the SEM that we need to do a better job of preventing nanoparticle aggregation if we are to realize the simulation conditions more accurately.

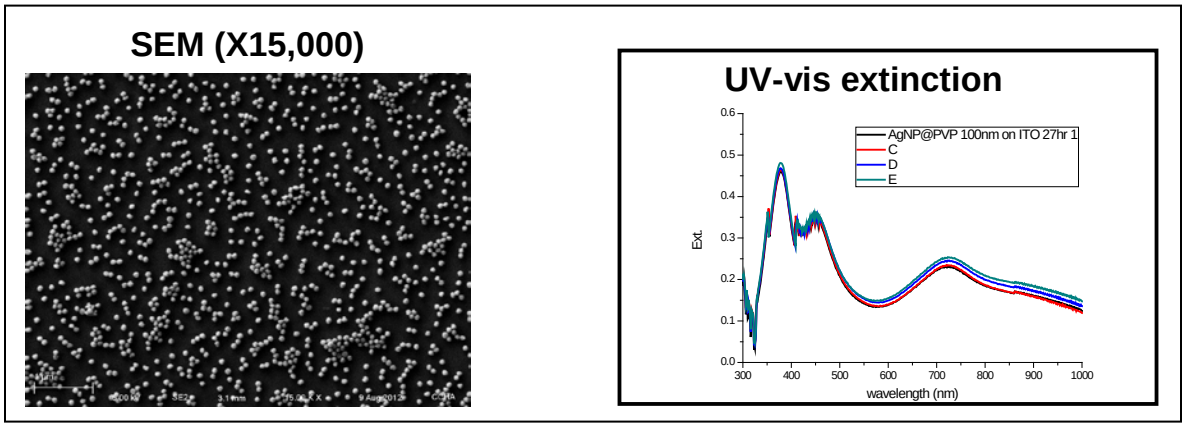

Figure 10. Scanning electron micrograph of self-assembled silver scattering layers (left) and UV-visible extinction spectrum (right).

By varying the exposure time of the substrate to the silver nanoparticle suspension, the optical density could be tuned from 0 to more than 0.5 (original milestone 4) or more. The deposition method we are using should be easily scalable to larger substrates and we consider the year 1 portion of our work to be completed satisfactorily. In year 2, we had planned to investigate ways to combine the particle deposition and planarization steps for a variety of reasons that will be discussed below.

D. Planarization of the scattering layers

Planarization was originally a year 2 task but was accelerated as discussed above. The purpose of the planarization is twofold. First, we want to "extend" the device waveguide so that light samples the scatterers effectively. This enables us to keep the scatterers out of the delicate electrical portion of the OLED that has been so carefully optimized with years of work. Second, the layer in which the scatterers are embedded needs to be planar with roughness much less than the thickness of OLEDs so that they can be grown on top effectively. It was our original idea that the refractive index of the planarization should be high to accomplish the waveguide extension function and relatively closely matched to the ITO anode refractive index so as not to introduce additional interfaces. For these reasons, we were originally aiming for planarization layers with refractive indeces between 1.8 and 2.0 although further modeling might suggest that lower refractive index could be better for spectral balance. Our choices of materials approaches reflect the desire for high refractive index. We felt that the simplest approach would be to develop TiOx sol gel chemistry to overcoat the silver layers and have used titanium tetrabutoxide in ethanol for the work shown below. An alternative approach would be to sputter high index dielectric (SiNx) and planarize with polymer and this is being pursued in parallel.

The titania produces very flat layers with thickness controllable by spin rate. Spectroscopic ellipsometry documenting TiOx thickness and atomic force microscopy (AFM) documenting its flatness are shown below in Figure 11.

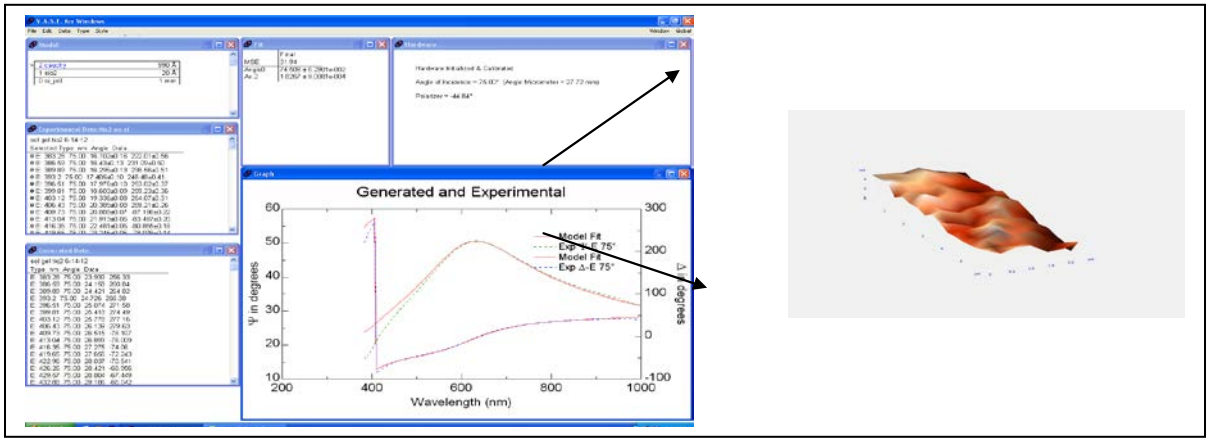

Figure 11. Ellipsometric data and analysis (left) and atomic force microscopy (right) for TiOx sol gel on glass.

The ellipsometry is combined with profilometry to measure the refractive index of the TiOx which turns out to be 1.83. The AFM measures rms roughness of ~ 2 nm which should be adequately flat to make good ITO and OLEDs. The data for high temperature polymeric coatings (cyclotene from Dupont) are similar except that the refractive index is closer to 1.60.

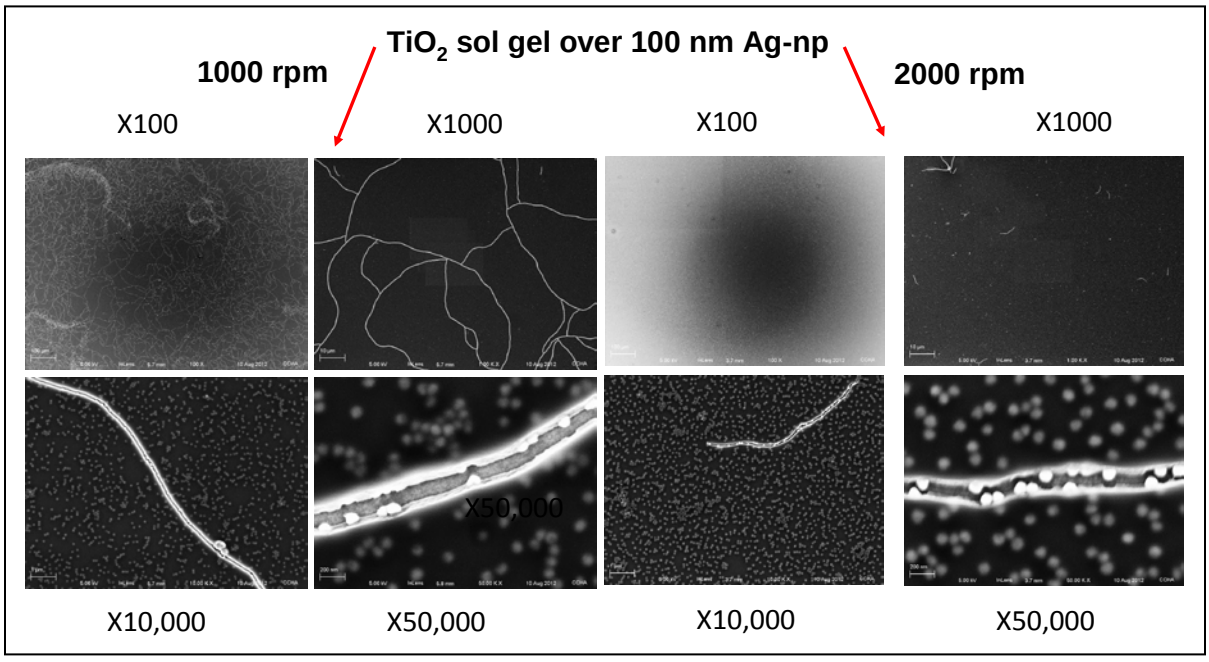

Figure 11. SEM picture of the TiOx over Ag nanosphere scattering layers under two different sol gel deposition conditions.

Unfortunately, the situation in TiOx is complicated when planarizing over silver nanoparticles. While we get large, flat domains, there is also a small amount of cracking that can be observed upon annealing (Figure 12) in scanning electron micrographs of the films.

Fully addressing the planarization problem will take longer but it is reasonably clear from literature that this problem can been solved adequately for our purposes. Due to pressure to have a year 1 demonstration of enhanced light extraction from OLEDs, we chose to defer this problem while simultaneously beginning to use the best of the planarized scattering layers we can fabricate to make model optical extraction and OLED measurements (see sections E and F respectively). At the same time, eMagin is developing the polymeric planarization documented in Figure 12 where crystallization (and the attendant cracking) cannot occur.

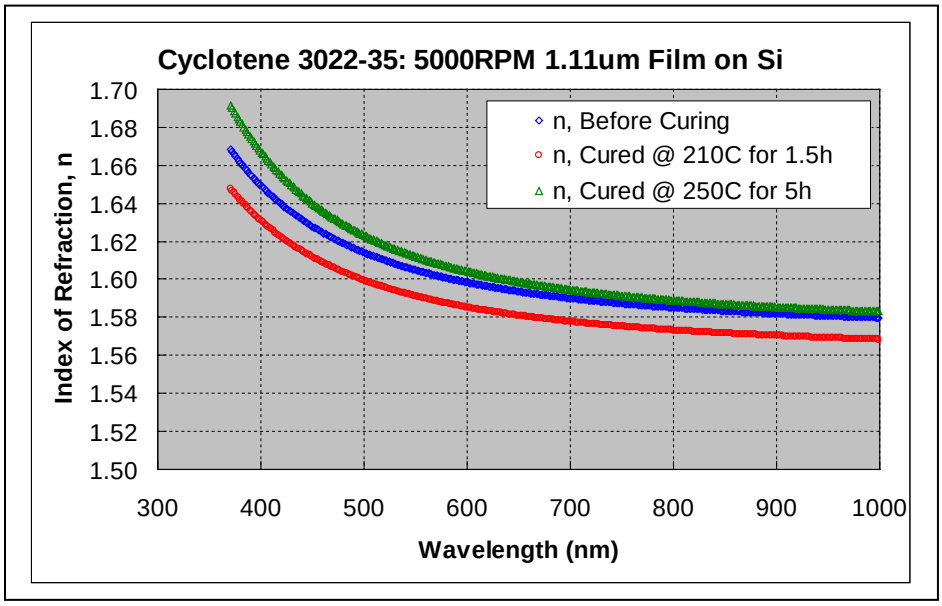

Figure 12. Refractive index measurements on the polymer planarization layer (cyclotene) under consideration.

We essentially accomplished our goal to planarize the layer containing the silver scatterers in a high index dielectric. We still need to address the cracking problem to make optimal devices and optical measurement structures on top of the layers (section E). We had hoped to investigate more three dimensional scattering layers where we incorporate the silver nanoparticles into the solution from which we deposit the planarization layer with the idea of both simplifying the process and reducing interparticle interactions to achieve finer control over the extinction spectrum.

E. Measurements of waveguide suppression in model structures and OLEDs

In our proposal, we designed simple proxy structures that we believed would enable us to demonstrate the efficacy of our scattering layers in outcoupling light from OLEDs without the need to make complete devices. These would simplify screening of scattering layers and comparison with theory even though we fully understand that they are not perfectly analogous. Before discussing our efforts to fabricate OLEDs on the scattering layers, we present the results of a measurement of suppression of total internal reflection in a prism geometry (milestone 9 of our original proposal slated for year 2), the relevance to

outcoupling from OLEDs being obvious. The experimental arrangement is shown schematically below as Figure 12 and was implemented with a nearly white source from a fiber laser and photonic gap fiber.

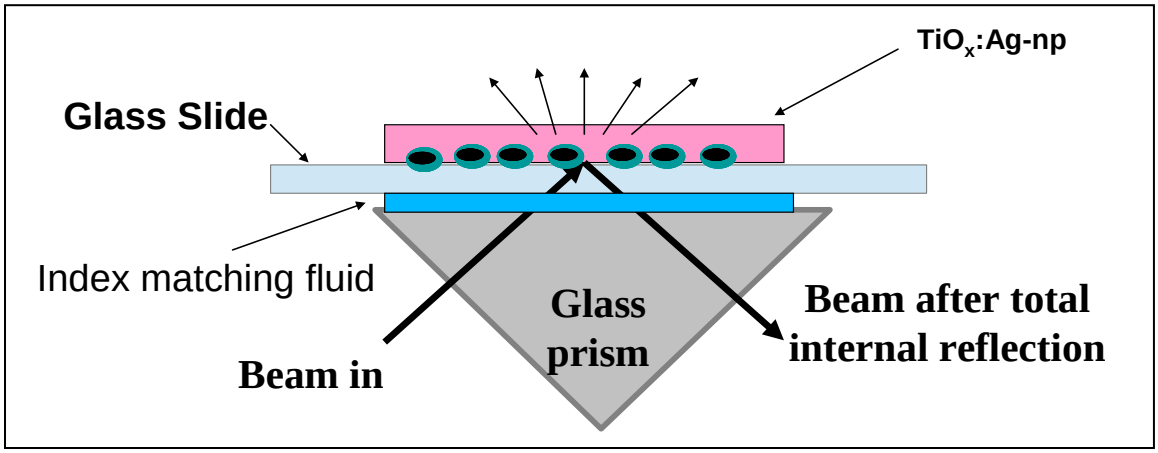

Figure 13. Measurement of suppression of total internal reflection by our silver nanosphere scatterers planarized with TiOx.

The glass slide was patterned so that only part of it contained the silver nanoparticle scatterers and the intensity of light reflected from the glass/air interface was measured with a calibrated photodiode in the regions without the scatterers (0.55 mW) and with the scatterers (0.06 mW). The fact that 90% of the light is lost is extremely encouraging though it is not straightforward to separate forward scattering out of the prism, backward scattering (which presumably would result in reflection from the cathode in an OLED) and absorption. We also measured the spectrum exiting the top surface (Figure 14) and found it remarkably similar to the incident spectrum for most of our scattering films, also extremely encouraging as it suggests minimal absorption (which would be heavily biased to the bluer wavelengths).

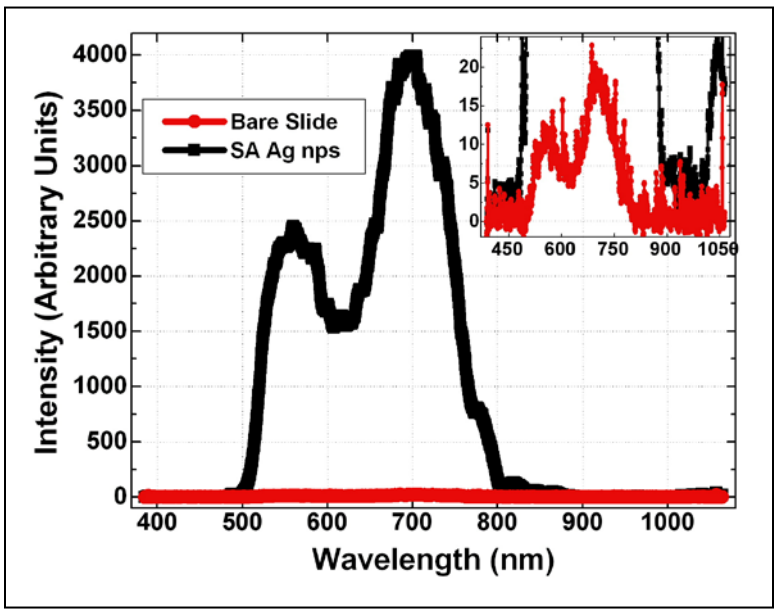

Figure 14. Light escaping the top surface in regions with a bare slide (red) and regions with a silver scattering layer. The bare slide data (expanded in the inset) show some scattering (probably from dirt) and are a good representation of the spectrum of the source.

In preparation for making OLEDs, we began to look at ITO sputtering on top of the planarization films. Figure 15 presents the results for growth on glass and these demonstrate our capacity to make excellent ITO. On TiOx, we have encountered the problem that the TiOx crystallizes under the conditions of best ITO growth and the attendant stress fractures the films (see section D). The resistivity and transparency meet the quality standards established by our metrics.

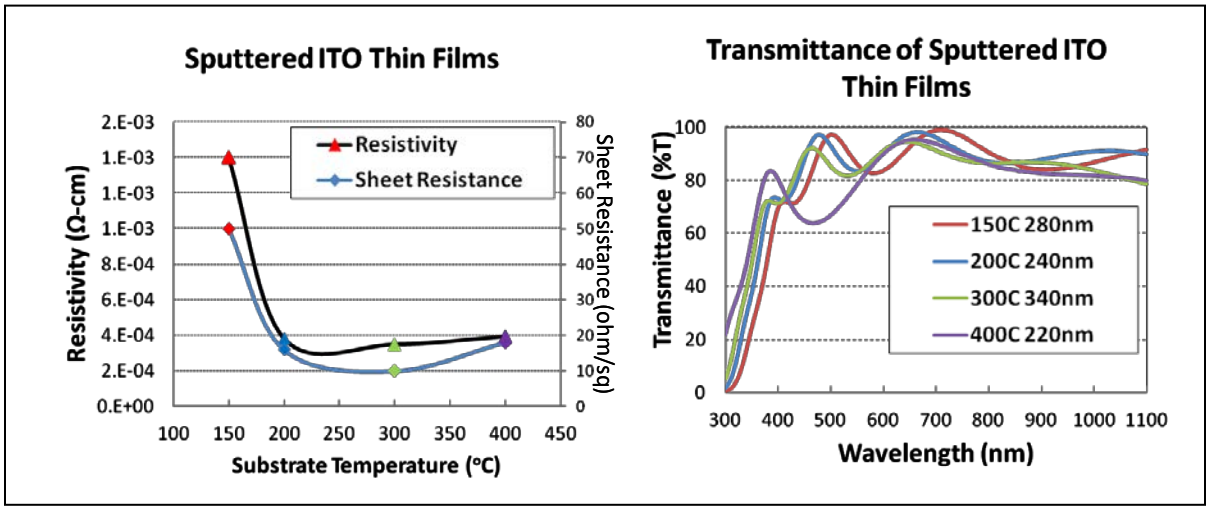

Figure 15. Resistivity and transmittance of 250 nm thick ITO sputtered in our coater.

F. Devices with plasmonic scattering layers

We did several runs where we made standard OLEDs (ITO only, "R series") and OLEDs on TiOx layers with homegrown ITO ("L-series") as controls and OLEDs where the TiOx was a planarization on top of silver nanospheres of ~ 100 nm diameter at around 20% coverage ("M-series"). A photograph of the substrates used is shown below as Figure 16.

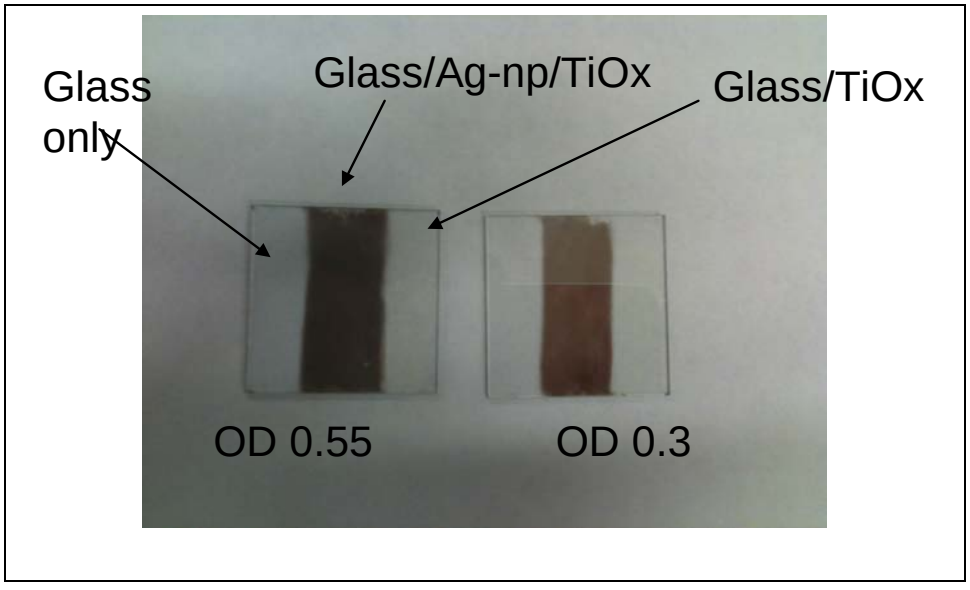

Figure 16. Substrate for OLED with scattering layers and controls.

The device data are summarized in the Table below.

Device	V	cd/m2	cd/A	EQE	CIEx	CIEy	Peak WL (nm)
L1	16.2	810	4.05	1.44	0.347	0.536	515
L2	15.7	313	1.57	0.51	0.369	0.520	566
L4	17.7	982	4.91	1.55	0.325	0.578	542
M1	13.9	407	2.04	0.68	0.362	0.536	535
M2	13.6	455	2.27	0.76	0.363	0.536	536
M3	13.7	437	2.19	0.73	0.361	0.537	534
M4	14.2	410	2.05	0.68	0.360	0.538	535
R1	13.8	579	2.90	0.94	0.340	0.562	537
R2	13.1	570	2.85	0.95	0.339	0.560	528
R3	13.2	588	2.94	0.96	0.336	0.564	534
R4	13.6	594	2.97	0.95	0.344	0.556	543
Alq Ref	7.8	809	4.05	1.27	0.360	0.555	537

Table 1. OLED results. Devices L have the structure TiOx| ITO |MoOx (3 nm) |NPB(150nm) |Alq3(50nm)|LiF:Al. Devices M have the structure TiOx:Ag:np| ITO |MoOx (3 nm) |NPB(150nm) |Alq3(50nm)|LiF:Al. Devices R have the structure ITO |MoOx (3 nm) |NPB(150nm) |Alq3(50nm)|LiF:Al. The Alq3 reference has 75 nm NPB and 75 nm Alq3.

We can draw a variety of conclusions from the data. First, there is probably not very much enhancement from the devices with silver scattering layers. This is not entirely clear because the most appropriate controls, the ones with ITO on TiOx (series L) did not function reliably and could be seen to be partially delaminating from the substrate causing high voltages and a fair amount of edge emission. However, the controls with no TiOx performed slightly better than the silver devices. In a way, it is encouraging that there is so little difference between the devices with the scattering layers and those without since it is clear from the photographs in Figure 16 that the silver is quite dark and if the darkness were largely due to absorption, the silver containing devices would be much worse than the controls. We have by no means optimized silver coverage, the silver particle size is smaller than predicted to be ideal by our simulations and the silver is not well dispersed (Figure 10), all addressable improvements.

Of additional interest is that we see small changes in the spectrum (Figure 17).

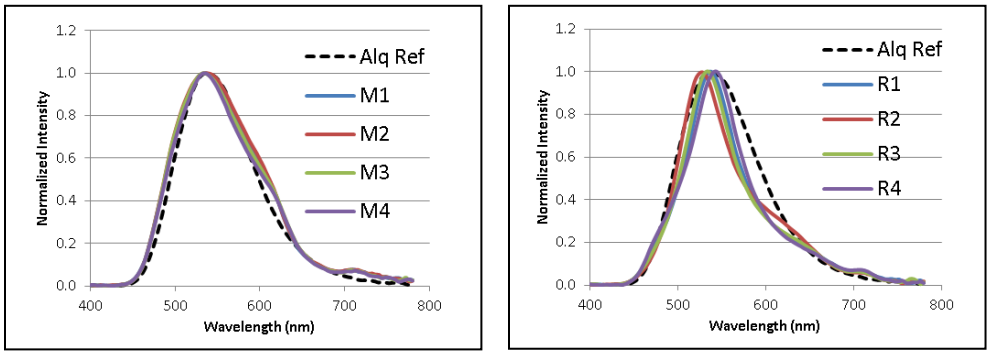

Figure 17. Electroluminescence spectra of the M series and R series devices from Table 1.

This observation enables us to reach two important conclusions. First, there may be extraction enhancement in the M series devices in the red portion of the spectrum which we would expect to be slightly better than the blue due to higher albedo of the scatterers. Second, the spectrum is not dramatically altered relative to the control devices across the entire range from ~ 460 nm to 650 nm. This bodes well for using plasmonic scatterers to outcouple light while maintaining reasonable color balance as required for solid state lighting.

A parallel effort to implement silver scatterers on top-emitting OLEDs was undertaken by eMagin. Their target device structure is shown as Figure 18 below where the cathode is a thin semitransparent metallic layer.

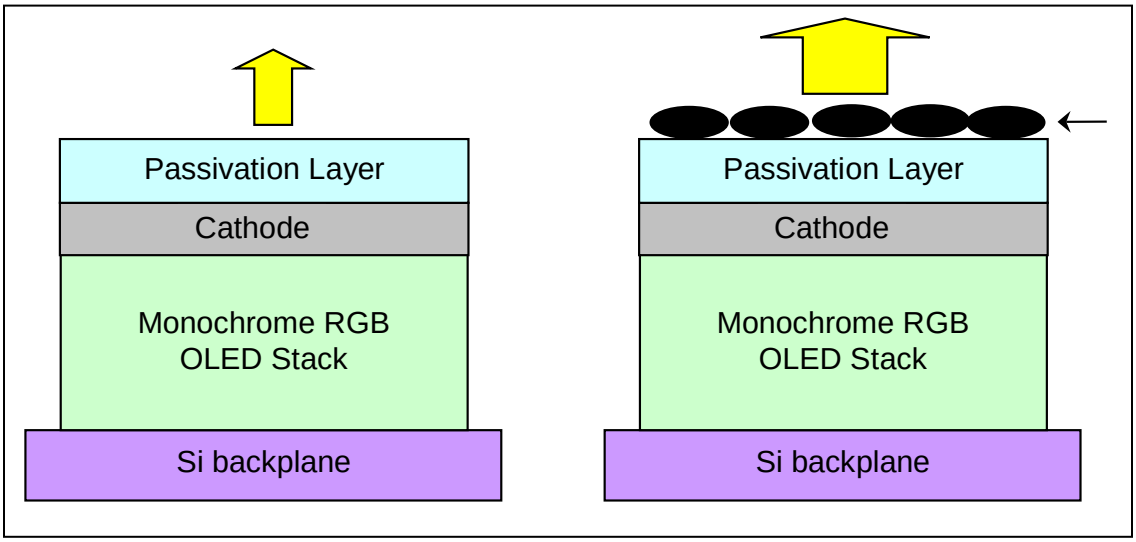

Figure 18. Top-emitting OLED structure.

In this case, a passivation layer was used so as not to damage the device and silver particles from a dry powder were deposited on top. Very little change in OLED efficiency was observed but unfortunately the silver coverages that were used were much too low to be expected to have any effect (OD ~ 0.03 at maximum extinction wavelength of 420 nm and < 0.01 in the visible spectral region) so these results remain inconclusive. We plan to continue to work on the theory and implementation of the top emitting devices at the University.

IV. Program achievements and learnings

Our key accomplishments are as follows:

1) Getting control of theoretical modeling and demonstrating that the premises of the program (strong scattering, low absorption for ≥ 100 nm diameter silver nanoparticles, broad resonance across the visible spectrum) are supported theoretically. Our calculations support modest enhancements but still have many degrees of freedom we have not exploited to improve structures. It may be necessary to tailor the particles further for improved forward scattering.

2) Synthesizing appropriate 100 nm diameter silver nanospheres with good yield and quality.
3) Assembling the silver nanospheres into 2-D assemblies using a simple, scalable process with the required extinction and with good optical density across the visible spectrum.
4) Coating the scattering layers with high refractive index planarization layers that can support ITO growth suitable for good OLED fabrication.
5) Demonstrating extremely efficient suppression of total internal reflection using our planarized scattering layers in a prism geometry.
6) Measuring extraction efficiency from OLEDs grown on planarized scattering layers. While we did not observe enhancement, we also did not observe much diminution of the extracted light in spite of using silver layers with very high extinction (OD > 0.3). Furthermore, we have not yet achieved optimal particle size or coverage nor adequately suppressed particle aggregation and so we anticipate improvements are possible.

V. Outlook for the future

To the best of our ability to do so, we plan to continue working on both the experimental and theoretical aspects of this project and to seek industrial support. Our theoretical work has convinced us that it is possible to achieve enhanced extraction and we continue to believe it is the single most highly leveraged problem to be solved if we are to make OLEDs viable for solid state lighting. Our experimental work is encouraging in that we are near break even using relatively dense nanotextured silver scattering layers that we know from the theory are not yet optimally configured in terms of size and dispersion of the particles.

VI. Budget

We were on track in terms of budget and cost share. These are appropriately documented in the separate non-technical report from the institution. Breakdown between categories should also be reasonably close to the original targets.